MODELLING HYDRODYNAMICS IN EELGRASS (*ZOSTERA MARINA*) BEDS

Jasper T. Dijkstra[1], Rob E. Uittenbogaard[2], Marcel J.F. Stive[1]

In many areas around the world, there is a large interest in the protection and restoration of aquatic vegetation, like eelgrass (*Zostera marina*), but little is known about the interaction of such vegetation with its environment. To improve this knowledge, a model has been developed that simulates this interaction between highly flexible vegetation and hydrodynamics. The model consists of two parts: a 1DV k-ε turbulence model that simulates the flow, and a model that simulates the movement of the vegetation, based on a Langrangian force balance. This model has been validated against our own measurements on positions and forces of flexible plastic strips, as well as hydrodynamic measurements from literature. It performs well in these situations, but the validation data is limited. Nevertheless, it can be considered to be a very useful and generic tool in studying flow processes in fields of flexible vegetation.

INTRODUCTION

The Dutch Wadden Sea is one of the areas where eelgrass (*Zostera marina*) almost disappeared in the 1930's. The cause of this disappearance it not really known, but it coincided with a combination of wasting disease, the closure of the Afsluitdijk and two subsequent years with a sunlight deficit (van Katwijk 2000). Eutrofication in the following decades may have hampered the return of eelgrass. Despite recent improvements in water quality and various small restoration efforts, the eelgrass population remains very small.

In larger quantities, submerged aquatic vegetation may act as an 'eco-engineer', i.e. it can alter its environment, so creating more favourable living conditions for itself and other organisms. In order to make future restoration attempts more successful, more insight is needed in this interaction between vegetation, currents, waves and sediment transport. Also in other areas, like e.g. the Chesapeake Bay (United States) and the Venice Lagoon (Italy), a more precise knowledge of eelgrass systems and their influence on sediment stability and ecological functions is considered useful, and subject of several studies (e.g. (Fonseca et al. 2002), (Amos et al. 2004)).

The flow through rigid vegetation is quite well understood, but the flow through and over flexible vegetation –like eelgrass- is different and less well known. The bending of plants allows for a greater flow over the canopy and a turbulence maximum closer to the bed, but the prone leaves can shield the bed and block the exchange of substances (Figure 1). The knowledge about these flow conditions can be gained from field and laboratory experiments, like the ones by (Nepf and Vivoni 2000), but these are often expensive and difficult to conduct. Moreover, empirical results have a limited range of applicability.

1 Hydraulic Engineering, Delft University of Technology, Stevinweg 1, 2628 CN Delft, The Netherlands
2 WL|Delft Hydraulics, Rotterdamseweg 185, 2629 HD Delft, The Netherlands

Therefore it seems logical to construct a computational model that is based on the processes that determine the interaction between flexible vegetation and its environment.

The processes defining this interaction are momentum exchange and bending of the plants. These processes are governed by a number of flow and vegetation parameters. Together with the buoyancy, the flow velocity distribution determines the force acting on the vegetation, hence the bending. But the bending also depends on the flexibility of the plant, which on its turn is defined by its cross section and elastic modulus. Then, the position of the plant influences the buoyant and hydrodynamic forces, and the circle is closed. Since these processes are basically the same for all types of vegetation, and the parameters can be measured for each species, such a process-based model is very generic.

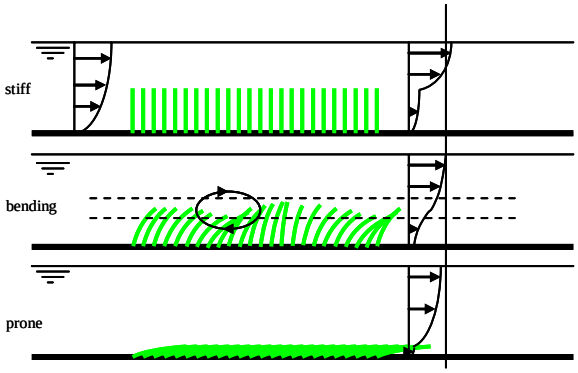

Figure 1 Flow velocity profiles in stiff, moderately flexible and very flexible vegetation

MODELLING OBJECTIVE AND APPROACH

The aim is to create a generically applicable tool that is useful in studying flow and flow related exchange processes in fields of different kinds of flexible vegetation, as well as hydrodynamic loads on the vegetation and the seabed. This means two models are necessary: one to simulate the hydrodynamics, and one to simulate the movement of the plants. Both models work fully implicitly for stability, whereas their interaction is explicit for calculation speed.

Though eventually a fully 3D simulation of a vegetation field will be necessary to incorporate all relevant hydrodynamic processes in and around a vegetation field, the most essential phenomena can also be investigated using a 1DV model. This model is an extension of the 1DV turbulence model for rigid vegetation as presented by (Uittenbogaard 2003).

A big difference with this earlier rigid vegetation model, is the fact that the movement of the vegetation also needs to be modelled. Due to the fact that eelgrass is very flexible, the plant deformations are too large to be adequately described by the standard equation for cantilever motion. Therefore, our method is to follow a Lagrangian approach by setting up a force balance of a leaf segment.

The vegetation model

Figure 2 shows the Lagrangian force balance per leaf segment. The distance measured along the leaf is *s*, at *s*=0 it is connected to the bed, $s=s_{max}$ is the tip of the leaf. On every leaf segment *ds* acts a distributed force *q* (N/m) as a result of its relative weight –which is very important in keeping aquatic vegetation upright-, combined with pressure and shear-stresses resulting from fluid motions relative to the velocity or acceleration of the segment. The force components *F* (N) act on the ends of the leaf segment. These are a combination of internal normal and shear stresses, integrated over the leaf cross section.

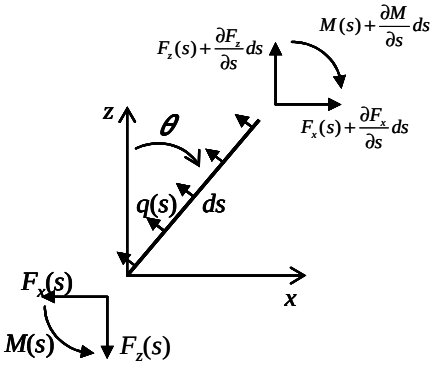

Figure 2 Force balance per element

The following limitations apply:

- A leaf moves in the vertical plane only. In reality it will always assume a position in accordance with the predominant flow direction, which is the direction imposed in the flow model.
- A leaf can only bend, and not elongate. Because eelgrass leaves are very thin, their moment of inertia is very small and thus bending dominates.
- A leaf cannot penetrate the bed.

The most prominent forces acting on the leaf are those due to pressure differences caused by turbulent wakes, but when the relative flow direction is nearly parallel to the leaf, also shear stresses need to be considered:

$$q_S = \frac{1}{2}\rho_w C_S b\left|\vec{u}_w - \vec{u}_v\right| u_S$$
$$q_N = \frac{1}{2}\rho_w C_N b\left|\vec{u}_w - \vec{u}_v\right| u_N \qquad (1)$$

Where q_S and q_N are the force components parallel and perpendicular to the leaf, respectively. C_S is the friction drag coefficient (actually, $C_S=fA_w$ with *f* a friction factor and $A_w=2(b+d)$ the wetted area of a leaf) and C_N is the coefficient for lift. Further, $\vec{u}_w$ and $\vec{u}_v$ are the velocity vectors of water and vegetation, and u_S and u_N the local velocity components with respect to the leaf. These velocity properties are determined by the hydrodynamic part of the model, ρ_w and *b* are constants, but the coefficients C_S and C_N are a source of uncertainty.

The reasons for this uncertainty are the dependency on the orientation with respect to the flow and the shape of the cross-section. Plenty of measurements are available for flat strips perpendicular or just almost parallel to the flow, but

nothing in between. Drag and lift coefficients along a range of angles could only be found for circular cross-sections, like in (Hoerner 1965). To clear this uncertainty, a series of experiments has been performed with strips of eelgrass-like dimensions at different angles with the flow. It is assumed that the coefficients found for a stiff strip under a certain angle, also apply to a series of small elements like in the model.

MEASUREMENTS: WHY AND HOW

The experiment has two objectives:

1. Obtain drag- and lift coefficients for strips with rectangular cross-sections at angles between 0 and 90 degrees, to be used in the flexible vegetation model;
2. Obtain validation material for this model, like forces and positions of flexible strips;

This required the following measurements:

1. Measure the horizontal and vertical forces on inflexible strips with eelgrass-like dimensions at different angles with the flow, along a range of flow velocities (Reynolds numbers).
2. Measure drag forces in combination with the position of strips of different flexibilities and different lengths, along a range of flow velocities.

Experimental setup

All measurements have been carried out in the racetrack flume (Figure 3) of NIOO-CEME (Netherlands Institute for Ecology – Centre for Estuarine and Marine Ecology) in Yerseke, the Netherlands. The flow in this flume is created by a drive belt, which is driven by a motor with a variable number of revolutions. Depending on the frequency of the transformer (0-60Hz), bulk velocities up to around 0.4 m/s are possible. The flume is 60 cm wide and can be filled with fresh or salty water to a depth of 40 cm. Collimators and screens in the bends regulate turbulence and bend effects. The test section is equipped with a transparent side wall to facilitate observations on specimen. In order to be able to determine C_N and C_S, and the influence of the angle of incidence and Reynolds number on these coefficients, the horizontal and vertical forces on inflexible metal strips have been measured. This has been done using strips of 5.0 mm width and 2.0 mm thin, with a rectangular cross-section and sharp edges. Producing thinner strips with sufficient stiffness and neat edges is difficult, and was not considered necessary because the flow pattern, hence the drag force, remains similar for these width/thickness ratios.

The angles (λ) of the strips ranged from 0 to 90 degrees, with increments of 10 degrees. For each angle, four strips were mounted onto the force transducer, see Figure 4. The use of four strips proved necessary because at low velocities, the force on a single strip turned out to be hardly measurable. The possible influence of strips on each other proved to be negligible.

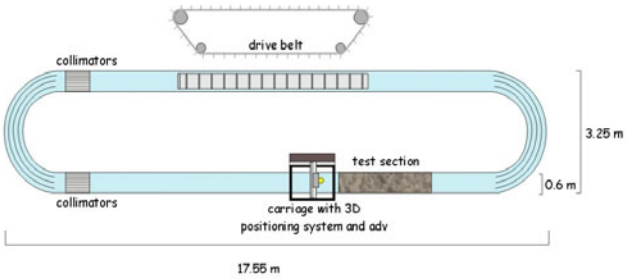

Figure 3 Top view of the race-track flume at NIOO-CEME. Flow direction is anti-clockwise.

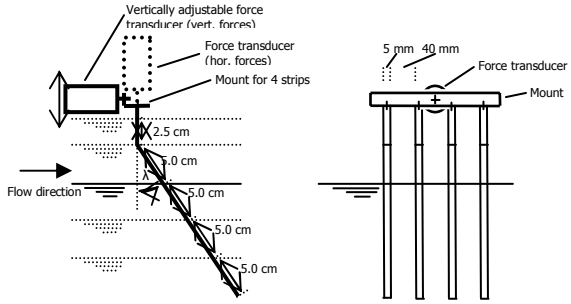

Figure 4 Strips mounted to the force transducer. Side view (left) and front view (right; looking upstream).

The forces using have been recorded a force transducer built by WL|Delft Hydraulics, at belt drive frequencies (i.e. velocities) of 10, 20, 30, 40, 50 and 60 Hz. In most cases, measurements were also taken at 5 and 15 Hz. Every recording, hence every raw data file, contains one minute of 20 Hz force measurements; i.e. 1200 values to give a good average. To rule out the effects of the tip and the water surface, the measurements took place at four 5 cm increments and a fifth 2.5 cm vertical piece, giving 5 measurements per strip. Measurements were done at the upper part of the water column to avoid the logarithmic velocity profile near the bottom, with the largest possible depth (40 cm) to get the most uniform velocity profile.

Instantaneous *u*, *v*, and *w* velocities at the measurement location have been measured for each drive belt setting (Hz) using an ADV, sampling at 25 Hz for 5 seconds. To obtain the representative bulk velocity at the location of the strips, instantaneous velocities have been averaged over time and over the area the strips occupied (Figure 5). Horizontal and vertical profiles over this area were quite uniform over this area, except for 5, 10 and 15 Hz.

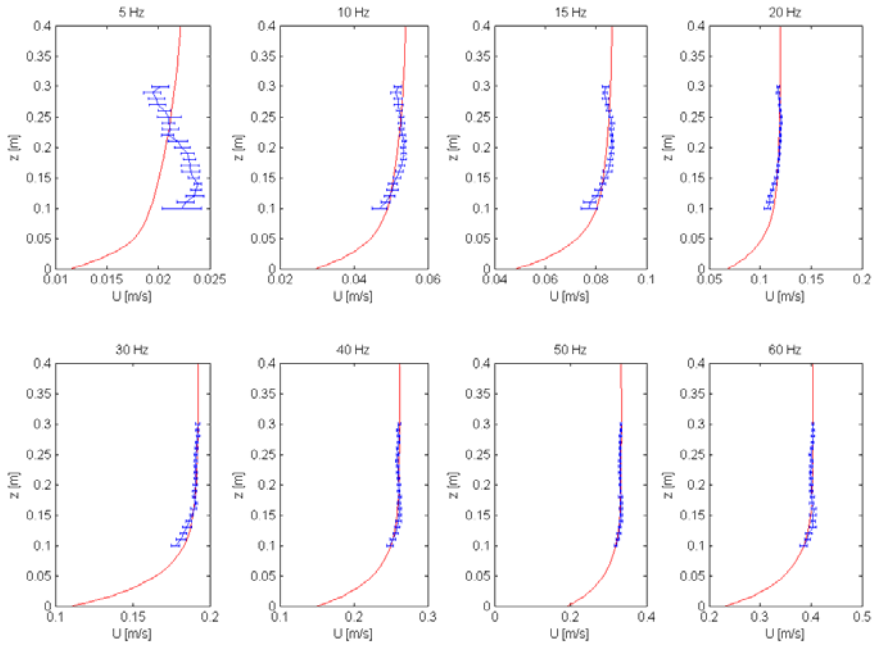

Figure 5 Velocity profiles, averaged over the measurement width. Note that for 5-15 Hz, the maximum velocity occurs well below the water surface.

Experimental results: coefficients

To derive the C_S and C_N as used in the model, the magnitude (F) and direction (β) of the total force are calculated from the measured horizontal (F_H) and vertical (F_V) force:

$$F^2 = F_H^2 + F_V^2 \tag{2}$$

$$\beta = \arctan\frac{F_H}{F_V} \tag{3}$$

Subsequently, the angle γ between the force angle β and strip angle λ has been calculated, which enables de decomposition of F in forces parallel (F_S) and perpendicular (F_N) to the strip:

$$\begin{aligned} F_S &= F\cos\gamma \\ F_N &= -F\sin\gamma \end{aligned} \tag{4}$$

Then, assuming only a horizontal velocity (i.e. w=0, u=u_H), C_S and C_N are defined according to:

$$C_N = \frac{F_N}{\frac{1}{2}\rho_w A u_H u_N}$$
$$C_S = \frac{F_S}{\frac{1}{2}\rho_w A u_H u_S} \quad (5)$$

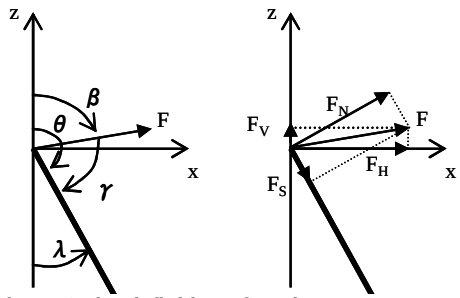

Figure 6 The definition of angles

In Figure 7 the values for C_S and C_N are plotted against the angle λ. According to the 'cross-flow' principle of (Hoerner 1965), the following is valid for circular cross-sections:

$$C_N = C_D \cos\lambda$$
$$C_S = fC_f \sin\lambda \quad (6)$$

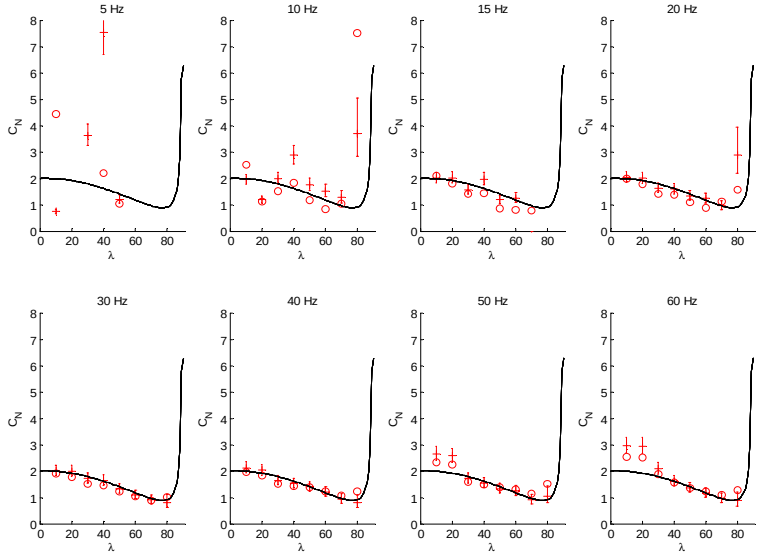

Figure 7 C_N as a function of angle λ. The circles are values corrected for tip effects, the crosses are uncorrected values with error bars, and the line is the fit according to Eq.(7).

Using equation (6) as a starting point for a fit would be obvious. However, in the case of C_N this is not possible; especially values at higher angles (i.e. a 'flatter' orientation) are much higher. The cause of this effect is not known, but if it is assumed to increase with the angle, a fit can be made using:

$$C_N = \min(2\cos\lambda + 0.1\tan\lambda, 2\pi)$$
$$C_S = 0.018 f \sin\lambda \quad (7)$$

With $f = Awet/A = 2.8$. In the model, C_N is limited to 2π for stability reasons, a value often used for plates at small angles of attack. The most useful measurements are those on 20, 30 and 40 Hz. At lower velocities, measurements are difficult and less accurate. At higher velocities, especially at small angles, the strips started to vibrate, resulting in a higher drag coefficient. Therefore, the values calculated for 30 Hz are used.

MODEL VALIDATION

Plant position and forces

Whether the position of the plant and forces acting on it are calculated correctly, can be checked by comparing the values predicted by the model with the measurements done at NIOO Table 2. These measurements have been done on three different types of strips, at different lengths and flow velocities, see Table 1. The positions (Figure 8) have been recorded using two 1-cm grids at the flume walls, marking the position on a transparent sheet.

Note that measurements at especially 5 Hz (2.0 cm/s) and also 10 Hz (5.0 cm/s) are likely to be less accurate (Figure 5). Furthermore, at high flow velocities strips started to vibrate, possibly resulting in a different drag coefficient, which has not been incorporated into the model. Analysis of possible errors in equipment, experimental set-up and the determination of strip properties made clear that the measured forces have an accuracy of 11%.

Table 1 Flexible strip properties. The E-modulus has been determined with a Perkin Elmer DMA 7e dynamic tester, the thickness with a micrometer and the width with a digital calliper.

strip	material	E (N/m^2)	thickness (m)	width (m)	I (m^4)	density (kg/m^3)
very flexible (FR)	PVC	1.60e9	1.78e-4	5.0e-3	2.30e-15	975
tie-wrap (TW)	Nylon 66	1.06e9	1.009e-3	4.8e-3	4.11e-13	1080
flexible transparent (FT)	copolyester	1.81e9	5.40e-4	5.0e-3	6.56e-14	1380
stiff transparent (ST)	copolyester	1.72e9	9.81e-4	5.0e-3	3.93e-13	1290

Table 2 Forces and relative errors. For measurements marked with #, the strips vibrated, ~ means a measurement error, and values marked by * are too low, probably as a result of a lower flow velocity in the upper part of the water column that could not be measured. The values are considered too low, since the maximum increase in force with respect to the other strip lengths is higher than theoretically possible.

U (cm/s)	L (m)	FR			TW			ST		
		F_{model} (10^{-2} N)	F_{exp} (10^{-2} N)	Error (%)	F_{model} (10^{-2} N)	F_{exp} (10^{-2} N)	Error (%)	F_{model} (10^{-2} N)	F_{exp} (10^{-2} N)	Error (%)
2.0	0.127	0.03	0.05	-33.9	0.03					
2.0	0.177	0.03	~0.03	28.6						
2.0	0.227	0.03	0.05	-30.0	0.05	0.06	-19.4			
5.0	0.127	0.11	0.12	-2.9	*0.18	0.15	21.6	0.19	*0.11	70.6
5.0	0.177	0.10	0.10	0.9				0.26	0.26	-2.2
5.0	0.227	0.10	0.10	-7.0	0.31	0.34	-7.6	0.33	0.34	-2.7
8.1	0.127	0.19	0.22	-13.5	0.46	0.00				
8.1	0.177	0.18	0.20	-9.4						
8.1	0.227	0.18	0.23	-20.9	0.80	0.79	1.6			
11.4	0.127	0.29	0.28	4.0	*0.89	0.76	17.8	0.93	*0.78	19.7
11.4	0.177	0.28	0.29	-0.2				1.28	1.27	0.9
11.4	0.227	0.29	0.33	-12.3	1.48	1.36	8.9	1.60	#1.65	-3.1
18.3	0.127	0.54	0.48	12.6	2.27	1.74	30.5	2.38	*2.05	15.9
18.3	0.177	0.56	0.49	12.5				3.18	#3.22	-1.5
18.3	0.227	0.58	0.53	9.1	3.08	2.89	6.7	3.62	#4.18	-13.6
25.0	0.127	0.82	0.72	14.4	4.06	3.29	23.3	4.34	*4.26	1.9
25.0	0.177	0.86	0.76	12.9				5.38	#6.32	-15.0
25.0	0.227	0.90	0.80	11.8	4.47	3.57	25.4	5.50	#6.51	-15.4
31.8	0.127	1.16	0.97	19.9	6.17	4.81	28.3	6.80	6.84	-0.6
31.8	0.177	1.22	1.04	17.3				7.63	#9.00	-15.3
31.8	0.227	1.27	1.06	19.3	5.86	4.22	38.8	7.29	#7.33	-0.5
38.6	0.127	1.53	0.98	55.5	8.25	6.48	27.2	9.42	10.24	-8.0
38.6	0.177	1.61	1.07	49.6				9.68	#10.38	-6.7
38.6	0.227	1.67	1.09	53.6	7.28	4.93	47.5	9.02	-8.18	10.2

Generally, keeping in mind that the accuracy in the force measurements is 11% and in the positions 0.5 cm, the results are pretty good. Despite predicting absolute values that are on average more than 11% off, the model certainly shows very much the same behaviour as the measurements.

The performance of the model at the lowest velocities is difficult to determine, since the forces are close to the sensitivity of the equipment, and the velocity profiles are far from uniform. Nevertheless, the results are not far off, though generally under predicted. This difference might be explained by the drag- and lift coefficient's independence of the Reynolds number in the model, whereas the measurements on stiff strips clearly indicated higher values at these low Re-numbers.

Apart from some individual anomalies, the structural differences in both force and positions between the model and reality can be explained by a possible dissimilarity of the velocity profile: In the model, the velocity is uniform over the upper part of the water column, whereas in reality it might be slightly lower

close to the water level. So close to the fixed end of the strip, this hardly affects it's bending, but it does lower the force to the square. On the other hand, if the velocity at the tip is slightly higher, the position will be strongly affected due to the larger leverage, and due to this more streamlined position, the increase in force is minimal.

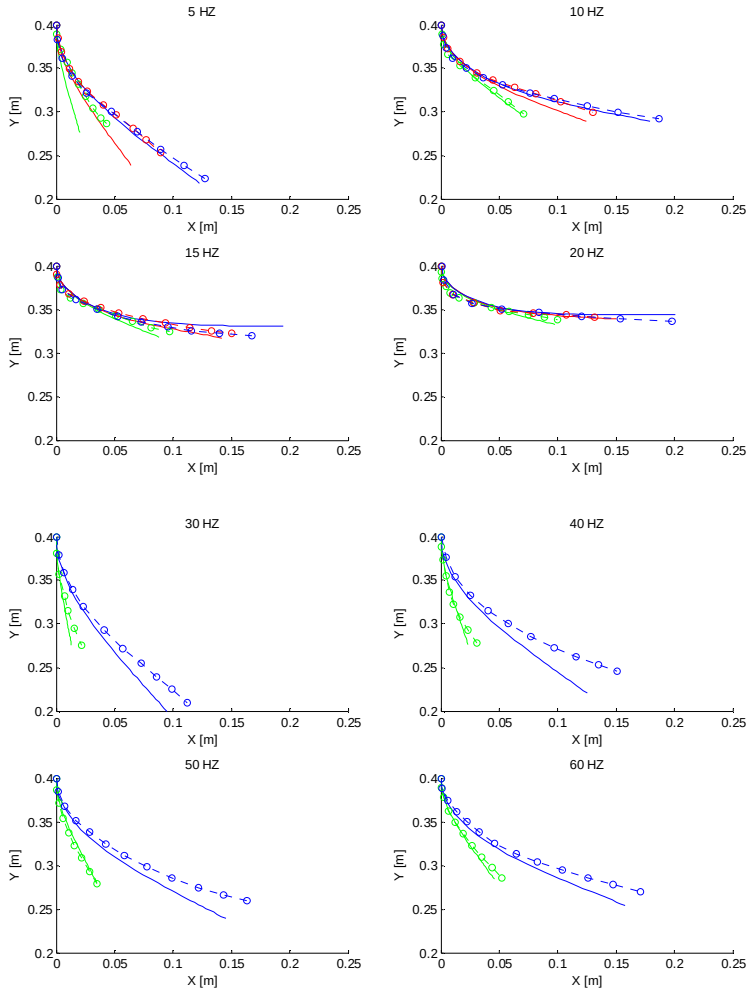

Figure 8 Measured (dotted lines) and modelled positions (continuous lines) from (a) the very flexible and (b) the tie-wraps at different velocities.

The structural under prediction of the forces and positions for the stiff transparent strips (Table 2, marked by '#') might be attributed to the drag increasing flutter, a phenomenon that is not incorporated in the model. The measurements on the stiff metal strips clearly show an increase (about 25%) in

drag if flutter occurs. Accounting for this 25% linearly, one comes to a 10-15% overestimation of the forces, which is similar to the other strips.

Hydrodynamics

To validate the hydrodynamic performance of the model, the results from (Nepf and Vivoni 2000) have been used. In their experiment, a 24 m long and 0.38 m wide flume was used, with a 7.4 m long canopy section. consisting of 330 randomly placed 0.16 m high plants per m^2, each made of six 3 mm wide, 0.25 mm thick vinyl blades attached to a 2 cm high wooden base (6.4 mm diameter). The elastic modulus of the blades is $2.56 \cdot 10^9$ Pa, the density of the material is not mentioned, but estimated at 975 kg/m^3. The best recorded experiment is for a flow depth of 0.44 m and a depth averaged velocity of 0.10 m/s.

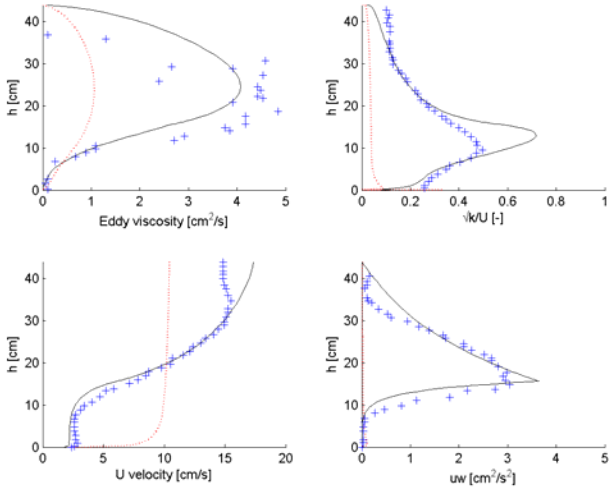

Figure 9 Profiles of hydrodynamic properties measured by (Nepf and Vivoni 2000) (crosses), predicted by the model (continuous line) and, for comparison, in case of absence of vegetation (dotted line).

Figure 9 shows the results of the experiment and model simulations. The agreement is fairly good, especially in the vegetated part of the water column. The discrepancies near the water surface are probably the result of secondary flows caused by side wall friction in the rather narrow flume, which are not incorporated in the model. Despite the fact that the plants do not bend very much in this situation, the model performs less well if the plants are modelled rigidly. In that case the production of turbulence, especially at the top of the vegetation, is far too high. This can be reduced by choosing a smaller drag coefficient, but the advantage of the flexible vegetation model is that it does not need any tuning, which demonstrates its general applicability.

DISCUSSION

Model performance

Despite some differences, of which the majority is explainable, the model performs well in both predicting the position of the vegetation as the hydrodynamic properties. The validation data is limited however, and the hydrodynamic performance is only validated in rather common flow conditions. To be really sure of its performance, it should also be tested in more extreme situations: higher and lower flow velocities, more flexible vegetation, different relative flow depths and different vegetation configurations.

Applicability

With the model in its current form, one can look in detail at processes in and above a vegetation field, and derive properties that govern the exchange of substances. Also it is possible to use the model as a predictor of bed roughness coefficients for areas with flexible vegetation like estuaries and floodplains, to be used in hydrodynamic models that do not account for vegetation explicitly.

Apart from its application to a specific situation, the model will also be used to generate a large dataset of artificial 'measurements'. With such a dataset and techniques like artificial neural networks or genetic programming, it is possible to derive general relations between flow and vegetation properties to facilitate easier and faster calculations in large-scale simulations.

Extensions

Of course, the most useful extension is to make the model multi-dimensional so spatial processes can be studied. In principle, this is not very difficult, as all the relevant processes are included, and the same extension to 3D has been made before for rigid vegetation.

Another very useful, but certainly more cumbersome, extension is to incorporate the interaction of flexible vegetation with waves. We feel sure that the motion of the vegetation in uniform flow is modelled reliably, and the vegetation model should perform equally well for wave motion, but here validation material is even more limited, and simulating waves in a 1DV model requires some simplifications.

In the current version of the model, the plant properties, like the cross-section, cannot be varied along the length of the plant. For short and simple plants like eelgrass this is not essential, but for larger plants that have larger variations along their length (e.g. large leafs), this is a very useful extension.

The plants in (Nepf and Vivoni 2000) are still almost upright, so it is interesting to compare model with data from more curved plants. In such a case it may turn out to be necessary to incorporate a mechanism that accounts for the horizontal position of the leafs that limits vertical exchange.

CONCLUSION

It can be concluded that the model performs well. Its achievement in determining the position and forces of strips of three different materials, at various lengths and flow velocities, indicates that the model and the drag/lift

coefficients are generally applicable. Also the hydrodynamic performance of the model is good, which means we have a very useful and generic tool in studying flow and exchange processes in and around fields of flexible vegetation. However, at the moment the model is only one-dimensional, and it needs to be validated further. Since good validation data is limited, we encourage experimental researchers to gather more data.

ACKNOWLEDGEMENTS

We thank NIOO-CEME for the use of their experimental facilities and Ben Norder of DelftChemTech for determining the properties of the artificial vegetation.

REFERENCES

Amos, C. L., Bergamasco, A., Umgiesser, G., Cappucci, S., Cloutier, D., DeNat, L., Flindt, M., Bonardi, M., and Cristante, S. 2004. The stability of tidal flats in Venice Lagoon--the results of in-situ measurements using two benthic, annular flumes. *Journal of Marine Systems*, 51(1-4), 211-241.

Fonseca, M. S., Whitfield, P. E., Kelly, N. M., and Bell, S. S. 2002. Modeling seagrass landscape pattern and associated ecological attributes. *Ecological Applications*, 12(1), 218-237.

Hoerner, S. F. 1965. *Fluid-dynamic drag*, Hoerner Fluid Dynamics, Vancouver.

Nepf, H. M., and Vivoni, E. R. 2000. Flow structure in depth-limited, vegetated flow. *Journal of Geophysical Research*, 105(C12), 28,547-28,557.

Uittenbogaard, R. E. 2003. Modelling turbulence in vegetated aquatic flows. *Riparian Forest Vegetated Channels Workshop*, Trento (Italy), 17.

van Katwijk, M. M. 2000. Possibilities for restoration of Zostera marina beds in the Dutch Wadden Sea, PhD thesis, University of Nijmegen, The Netherlands.